Neural compensation for the best aberration correction

Li Chen Center for Visual Science, University of Rochester, Rochester, NY, USA

Pablo Artal Laboratorio de Optica, Universidad de Murcia, Murcia, Spain

Denise Gutierrez Hartnell Community Collage, Salinas, CA, USA

David R. Williams Center for Visual Science, University of Rochester, Rochester, NY, USA

We use adaptive optics (AO) to study whether neural adaptation influences the amount of higher order aberration correction that produces the best subjective image quality. Three subjects performed two tasks, method of adjustment and matching, while viewing a monochromatic stimulus through the Rochester AO system. In both tasks, after correcting the subject's lower order aberrations with trial lenses, AO was used to modify the subject's higher order aberrations, multiplying it by a scaling factor between 1 and −1. In the adjustment task, subjects adjusted the scaling factor to find the best subjective image quality. In the matching task, subjects viewed the same stimulus sequentially blurred either by defocus or a scaled version of their own wave aberration, adjusting the defocus to match the blur corresponding to different scaled versions of their aberrations. Results from both tasks are consistent with a small amount of neural adaptation because the best subjective image quality occurred when some higher order aberrations were left uncorrected for all three subjects. Neural adaptation slightly modifies the best aberration correction, although this effect averaged only ~12% of complete adaptation. These results may have practical consequences for customized vision correction.

Keywords: neural adaptation, physiological optics, optical aberrations, adaptive optics

Citation: Chen, L., Artal, P., Gutierrez, D., & Williams, D. R. (2007). Neural compensation for the best aberration correction. *Journal of Vision, 7*(10):9, 1–9, http://journalofvision.org/7/10/9/, doi:10.1167/7.10.9.

Introduction

The human eye suffers from wave aberrations that degrade vision. The lower order aberrations, defocus and astigmatism, have been measured at least 200 years ago (Young, 1801). These lower order aberrations are corrected with spectacles, contact lenses, intraocular lenses, and refractive surgery. Higher order wave aberrations, beyond defocus and astigmatism, have been known to exist in the eye for more than 150 years (Helmholtz, 1881). Since Smirnov (1961) used a psychophysical method to provide a description of the third and forth order aberrations, investigators have demonstrated a variety of different methods for estimating the wave aberrations of the human eye (Artal, Guirao, Berrio, & Williams, 2001; Campbell, Harrison, & Simonet, 1990; He, Marcos, Webb, & Burns, 1998; Hofer, Artal, Singer, Aragón, & Williams, 2001; Howland & Buettner, 1989; Howland & Howland, 1977; Iglesias, Berrio, & Artal, 1998; Liang, Grimm, Goelz, & Bille, 1994; Navarro & Losada, 1997; Mierdel, Krinke, Wiegand, Kaemmerer, & Seiler, 1997; Rosenblum & Christensen, 1976; Van den Brink, 1962; Walsh, Charman, & Howland, 1984). These pioneering studies greatly increased our understanding of the eye's higher order wave aberration. In recent years, the Shack–Hartmann wavefront sensor has become a popular method for wave aberration measurement with the goal of compensating these higher order aberrations to achieve diffraction-limited optics in the living eye (Fernández, Iglesias, & Artal, 2001; Hofer, Chen, Yoon, Yamauchi, & Williams, 2001; Liang & Williams, 1997) and customized vision correction with contact lens, intraocular lenses, and refractive surgery. However, the subjective image quality of the human eye depends not only on the optical blur caused by the wave aberrations but also on neural factors and the experience of the observer (George & Rosenfield, 2004; Mon-Williams, Tresilian, Strang, Kochhar, & Wann, 1998; Pesudovs & Brennan, 1993; Rosenfield & Hong, 2001; Rosenfield, Hong, & George, 2004; Watt, 1987; Webster, 2005; Webster, Georgeson, & Webster, 2002). This fact is well known among clinicians who often use a two step procedure to achieve a full correction of astigmatism, allowing time between the two steps for the patient's nervous system to adjust to a partial correction. There is adaptation not only to defocus and astigmatism, but also to the particular pattern of higher order aberrations (Artal et al., 2004). The subjective blur produced when viewing a scene through one's own wave aberration was less than that when the wave aberration was rotated. In the present paper, we investigate whether this neural compensation

doi: 10.1167/7.10.9 Received November 16, 2006; published July 23, 2007 ISSN 1534-7362 © ARVO

modifies the amount of aberration correction that produces the best subjective image quality.

Methods

Subjects

Measurements were made on the right eyes of three subjects all in their second decade of life. All three subjects had normal vision. One subject was emmetropic and the refractive errors of the other two subjects ranged from −1 D to −2 D for sphere only. Only one subject wore spectacles with spherical correction only. During the experiment, the subject's head was stabilized with a dental impression, and the subject's pupil was dilated and accommodation reduced with tropicamide (1%). The lower order aberrations of each eye were corrected with trial lenses. The research followed the tenets of the World Medical Association Declaration of Helsinki, informed consent was obtained from the subjects after we explained the nature and the possible complications of the study, and our experiments were approved by the University of Rochester Institutional Review Board.

Experiment setup

Each subject viewed visual stimuli with his higher order aberrations controlled by an adaptive optics (AO) system. AO has been used to compensate the eye's higher order aberrations in vision science (Fernández et al., 2001; Hofer et al., 2001; Liang, Williams, & Miller, 1997). One application of this technology is to obtain high-resolution retinal images to resolve individual photoreceptors in vivo (Liang & Williams, 1997) and to identify the photopigment in each cell (Roorda & Williams, 1999). Another important application is to produce controlled wave aberration patterns in the eye, enabling new experiments to better understand the mechanisms of the vision system (Artal et al., 2004; Chen, Singer, Guirao, Porter, & Williams 2005). In this study, we used the Rochester AO not only to compensate the eye's wave aberration, but also to act as an aberration generator to deliberately blur the subject's vision.

Figure 1 is a schematic diagram of the Rochester AO system used in this study. A narrow infrared beam from an

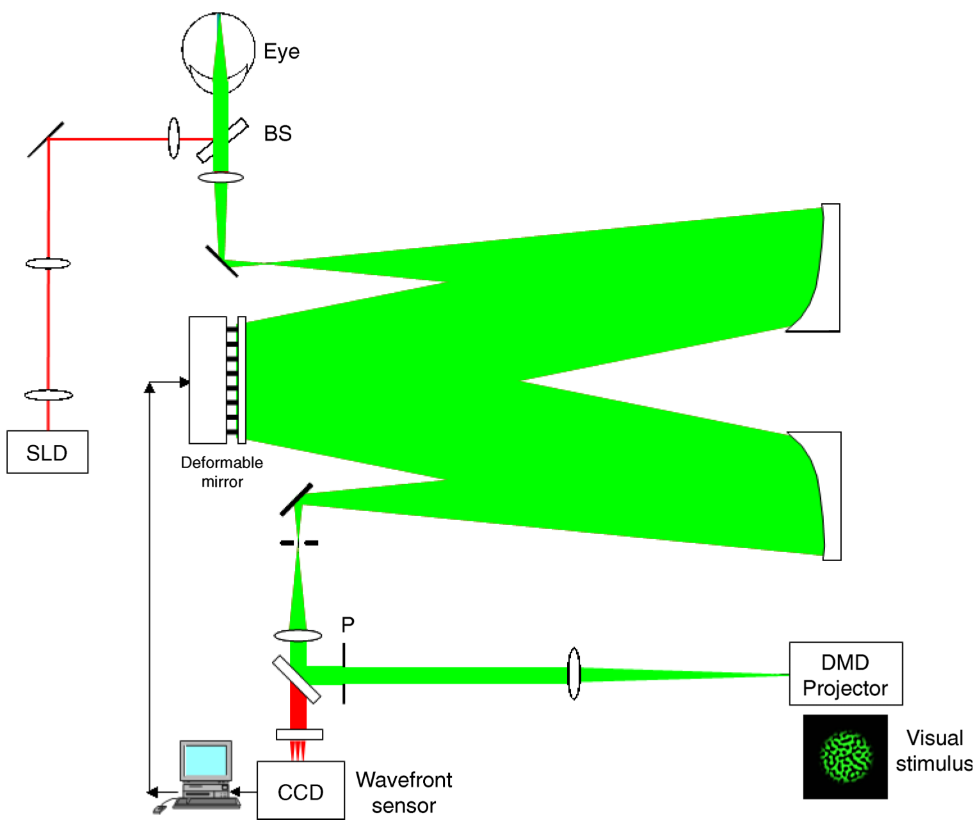

Figure 1. Schematic diagram of the Rochester AO system used in the experiments. The red path represents the infrared light used for measuring the wavefront aberration and driving the deformable mirror, whereas the green path is the light used for stimulus delivery. Although not shown for clarity, the paths are coextensive from the beam splitter (BS) after the eye to the cold mirror. See the text for additional details. CCD, charged-coupled device camera; DMD, digital micromirror device; SLD, super-luminescent source. The picture in the lower right corner represents the visual stimulus used in the experiment (see the text for additional details).

810-nm super-luminescent diode (SLD) is focused into the subject's retina. The irradiance of the SLD on the cornea was approximately 5 μW, which is about 30 times smaller than the maximum permissible exposure for continuous viewing according to the safety standards (ANSI Z136.1, 1993). After the beam is reflected from the retina and passes through the optics of the eye, a Shack–Hartmann wavefront sensor (Liang et al., 1994; Liang & Williams 1997), placed conjugate with the subject's pupil, measured the eye's wave aberration at 30 Hz. This wavefront sensor has 177 lenslets arranged in a square array, which could measure aberrations for a 6-mm pupil up to the tenth order, corresponding to 63 Zernike modes. A Xinetics deformable mirror with 97 PMN actuators, placed at one conjugate plane to the subject's pupil between the eye and the Shack–Hartmann wavefront sensor, is used to control the subject's wave aberration based on the measurements from the Shack–Hartmann wavefront sensor. This process is done in a closed-loop fashion so that the AO system is working at 30 Hz to fix the aberrations we want to their desired values. Because the stroke of the deformable mirror is not large enough for controlling all aberrations in some eyes, we used trial lenses placed in front of the eye to correct defocus and astigmatism, sometimes supplemented by an additional defocus adjustment provided by sliding the eye and lens closest to the eye together while keeping the distance between them fixed. The deformable mirror then compensated any residual low order aberrations as well as the higher order aberrations and generated the aberrations that we wished to present to the eye. For normal young subjects, the wavefront correction and the wavefront generation could achieve less than 0.07-μm wavefront error over a 6-mm pupil.

Subjects viewed a test field subtending 1° of visual angle through a 6-mm artificial pupil in the AO system. The stimulus, also shown on the bottom left in Figure 1, was displayed on a digital micromirror device (DMD). It contained a binary noise pattern with sharp edges at random orientations. A different noise pattern was used to generate a new stimulus on each trial so that edges at all orientations were presented over the course of the experiment. We chose this stimulus because its sharp edges make it easy to detect small amounts of blur. Moreover, the fact that all orientations are represented ensures that all aberrations, many of which tend to produce blur that varies with orientation, have an opportunity to influence image quality. The SLD stayed on during the experimental procedure for closed loop correction and wavefront generation. However, the SLD was aligned at the edge of the test field, so as not to disrupt sensitivity to blur. The SLD lay well within the isoplanatic patch size for AO correction (Williams, Liang, Miller, & Roorda, 1999), so that the quality of the correction was not compromised by the displacement of the SLD from the eye's fixation point. A negative trial lens was placed in the pupil plane (denoted with 'P' in Figure 1) between the cold mirror and the projector, and the lens in front of the projector was repositioned axially, to compensate for the −0.85-D chromatic aberration difference between the stimulus and the wavefront sensing wavelength of 810 nm. The retinal illuminance of the stimulus display was 390 Trolands measured with an IL17000 Radiometer.

Experimental procedures

Subjects performed two tasks, method of adjustment and matching, while viewing the stimulus through the AO system. In both tasks, the subject's lower order aberrations were corrected by trial lenses, whereas the subject's new higher order aberrations were his normal aberration multiplied by a scaling factor between 1 and −1. 1 corresponds to the normal wave aberrations, 0 corresponds to the wave aberrations minimized with AO, and −1 corresponds to the normal wave aberrations but with the sign reversed. The subject's normal wave aberrations were the average of 10 aberration measurements at the beginning of each trial.

The subject viewed the stimulus for 500 ms immediately after the deformable mirror generated the desired wave aberrations. In between stimulus presentations, the subject viewed a uniform field for 300 ms when the AO system was generating the desired wave aberrations in closed loop.

Procedure 1

Subjects were asked to adjust the scaling factor to find the best subjective image quality. On each trial, the deformable mirror was used to replace the subject's wave aberration with one of his scaled wave aberrations. Each trial consisted of two 500-ms intervals during which the binary noise stimulus pattern was displayed. During the first interval, the binary noise stimulus was viewed with a wave aberration corresponding to the subject's normal wave aberrations. During the second interval, the stimulus was viewed with wave aberrations corresponding to one of his scaled wave aberrations. Subjects then maximized the subjective image quality in the second interval by adjusting the scaling factor. The scaling factor was used to multiply the subject's normal wave aberrations, up to 10th order Zernike coefficients, to present a new scaled wave aberrations generated by the deformable mirror. The subject could adjust the scaling factor between 1 and −1 with a minimum step size of 0.1. To avoid possible adaptation to a new pattern of wave aberrations, we presented the subject's normal wave aberrations in the first interval of each trial. The scaling factor that maximized image quality was taken as the average of six measurements.

Procedure 2

A matching procedure was used to measure the subjective blur produced by scaled wave aberrations. The subject's task was to adjust the amount of defocus to match the subjective blur of the stimulus to that seen when the wave aberration was one of his scaled normal wave aberrations. In the matching process, one of the scaled wave aberrations was randomly selected. Subjects were asked to match the blur with defocus. Subjects could not tell which scaled wave aberration was presented on a given trial. Each trial consisted of two 500-ms intervals during which the binary noise stimulus pattern was displayed. During the first interval, the binary noise stimulus was viewed with wave aberrations corresponding to one of the subject's scaled wave aberrations. During the second interval, the stimulus was viewed with a defocus that the subject could increase or decrease in amplitude in steps of 0.05 μm. Figure 2 shows the matching procedure in which the subject changed the value of defocus to match the blur caused by one of his scaled wave aberrations. Defocus was chosen as the test aberration to quantify the blur caused by the scaled wave aberration because it is a familiar source of blur and its magnitude can be expressed conveniently in diopters.

The matching value of defocus to each scaled aberration was measured four times at the positive value and four times at the negative value. The final matching value was the average of the absolute values of these eight measurements.

Results

Figure 3 shows an example of the ideal case we sought to achieve with our AO system. It shows the wave aberrations with a scaling factor of 1 corresponding to the normal wave aberrations, 0 corresponding to the aberration-free case, and -1 corresponding to the negative of the normal wave aberration. Scaled 0.5 wave aberrations and -0.5 wave aberrations are the normal wave aberrations multiplied by scaling factors 0.5 and -0.5, respectively. The calculated point spread functions (PSFs) corresponding to each scaled wave aberration are shown in the middle row. The bottom row simulated the image quality of the stimulus viewed through the scaled wave aberrations by convolving the 1° test stimulus with the corresponding PSF in the middle row. The PSFs of the negative scaled aberrations have the same PSFs of the positive scaled aberrations rotated by 180°. The simulation shows that the scaling 0 wave aberration has the best image quality. The negative scaled PSFs produce a retinal image with an identical modulation transfer although with a different phase transfer function, as compared with the positive scaled PSF. The image quality for normal and negative scaling factors of the same absolute value has the same apparent image quality in the simulation with the stimulus we used in this study.

Figure 4 shows samples of the scaled wave aberration presented in one real eye with AO in which the wave aberrations was measured by the Shack–Hartmann wavefront sensor. The PSF of each scaled wave aberration is shown in the middle row. The bottom row images show the simulated image quality of the stimulus viewed through the scaled wave aberrations, obtained by convolving the

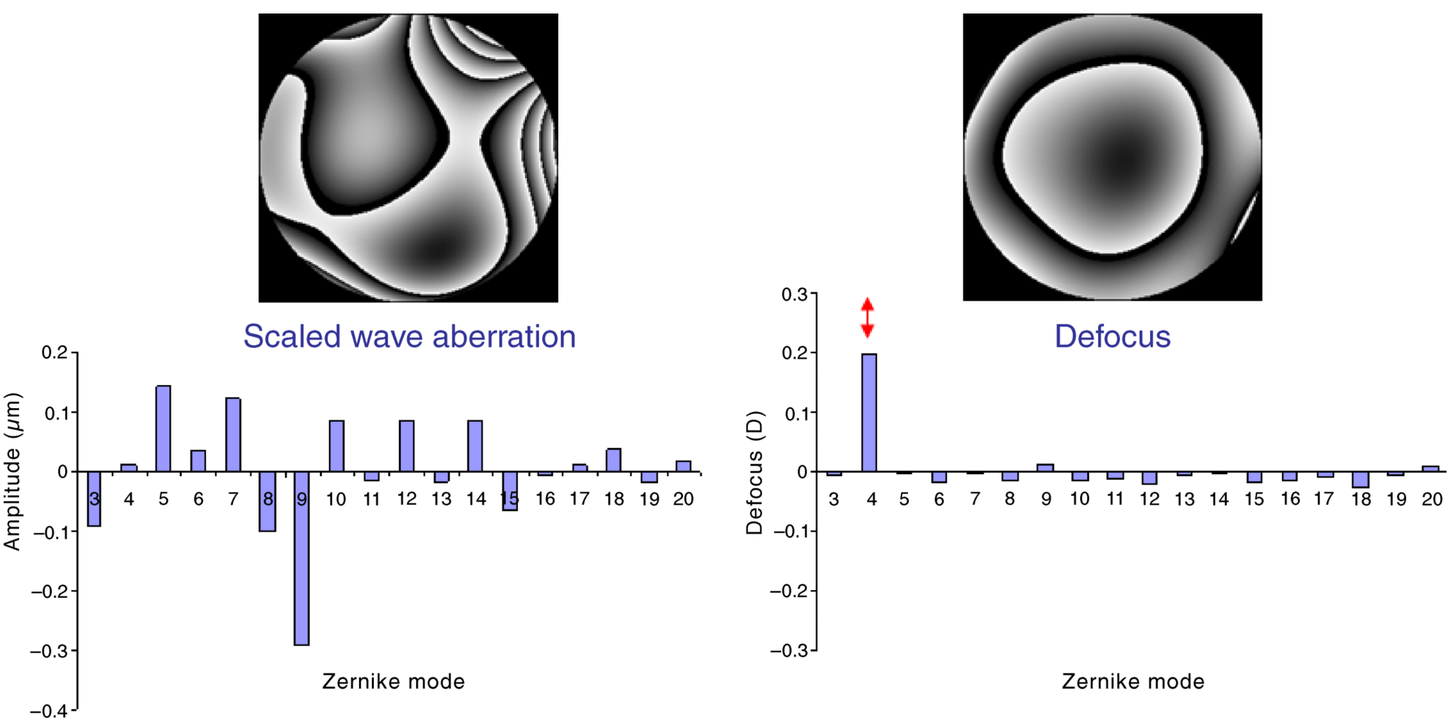

Figure 2. Experimental procedure of blur matching with the scaled wave aberrations. The subject alternatively viewed the stimulus through one of his scaled wave aberration generated by the AO system (top left) and through Zernike defocus (top right). The values of the scaled aberrations are shown in the bottom left. The amplitude of defocus could be adjusted by the subject to match the blur created by his scaled aberrations.

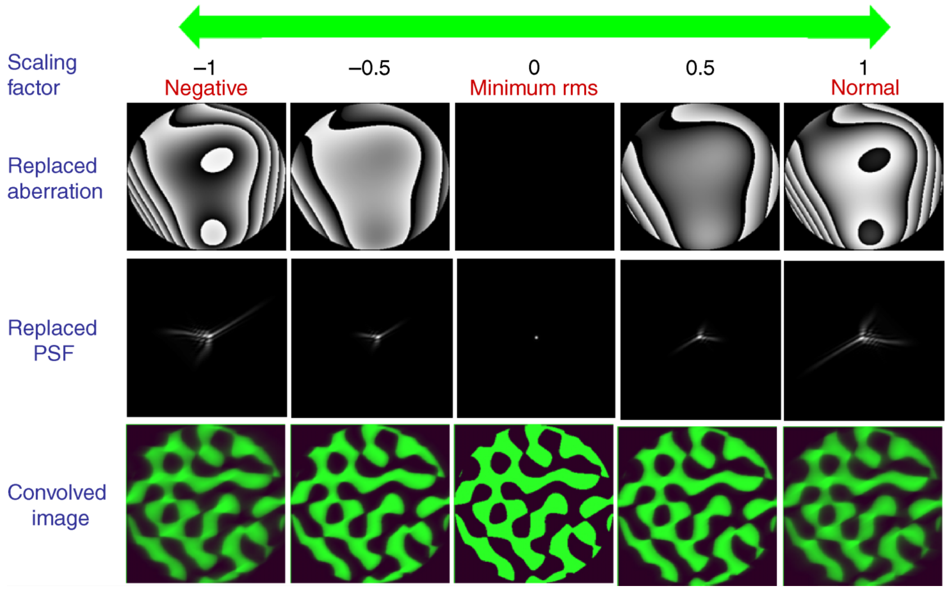

Figure 3. Simulated image quality from the scaled aberrations. At the top of this figure are examples of scaled wave aberrations from the simulation. In the middle row are the calculated PSFs, and the bottom row shows the convolved image from these PSFs. Each PSF image corresponds to 37 arcmin visual angle on a side.

1° tested stimulus with the corresponding PSF in the middle row. Here 0 corresponds to wave aberrations that were minimized by AO, with the residual aberrations between the targeted wave aberration and the wave aberration generated by AO corresponding to about 0.1 μm. The similarity between the corresponding normal wave aberrations and negative wave aberrations shows that the AO system did not have an intrinsic asymmetry in its ability to produce aberrations of different sign. That is, the simulation shows that the best image quality occurred when the scaling factor is zero and the image quality is the same for positive and negative scale factors of the same magnitude. That no asymmetry was present in the aberrations that were generated was important to confirm because the deformable mirror was nearly flat for scaling factors near 1 and was increasingly deformed as the

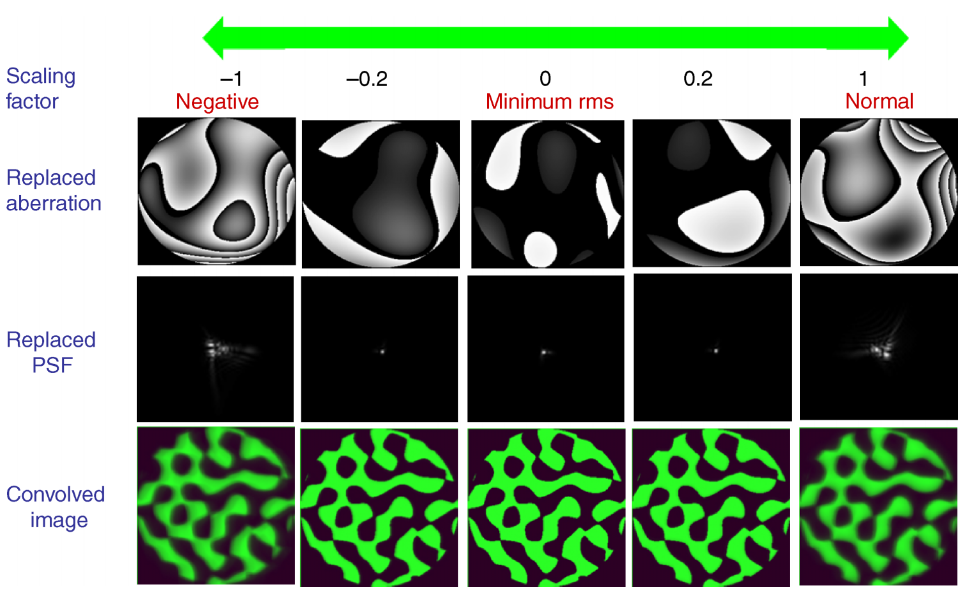

Figure 4. Scaled aberrations generated by AO. At the top of this figure are samples of scaled wave aberrations from one subject generated in one real eye with AO. The middle row shows the calculated PSFs, and the bottom row shows the convolved image from these PSFs. Each PSF image corresponds to 37 arcmin visual angle on a side.

scaling factor was reduced toward −1. Eventually, when the maximum stroke of the deformable mirror is reached, asymmetries are inevitable. We avoided such asymmetries by using young subjects with relatively small amounts of higher order aberrations. The average wavefront error across these three subjects was 0.40 μm with a 6-mm pupil. Subject DG had about 0.12 μm vertical coma, 0.1 μm trefoil, and 0.1 μm spherical aberration. Subject GP had very modest higher order aberrations, such as less than 0.12 μm trefoil and 0.08 μm spherical aberration. Subject LW had relatively larger third order aberrations among these three subjects. The dominant aberrations from subject LW were 0.22 μm vertical coma and 0.2 μm trefoil.

Figure 5 shows the results from the method of adjustment. All observers chose a scaling factor significantly greater than zero, ranging from 0.03 to 0.18. The best subjective image quality occurred when the wave aberration was shifted slightly in the direction of the normal wave aberration, with a mean value of 0.12 in the three observers. This is consistent with some neural adaptation because the best image quality occurred when some aberrations are left uncorrected in all three subjects.

Figure 6 shows blur matching results averaged across the three subject's measurements. For the matching task, each of the three subject's data revealed a small amount of neural adaptation because the amount of defocus required to match subjective image quality was minimal for aberration factors slightly greater than zero. This result is also consistent with a small amount of neural adaptation because the amount of defocus required to match subjective image quality is minimal for aberration factors slightly greater than zero. The fitting curve shows that the lowest matching defocus, corresponding to the best subjective image quality, occurred at 0.12. During the matching procedure, subjects reported that matching was not always possible when the scaling factor was between near that which produced the best perceived image quality. This was because the perceived image quality was sometimes better for the test stimulus than for the matching stimulus seen with through minimized aberrations and zero defocus.

Discussion

A previous study demonstrated that the eye is adapted to its particular pattern of higher order aberration because the subjective blur produced when viewing a scene through one's own wave aberration was less than that when the wave aberration was rotated (Artal et al., 2004). In this study, by presenting scaled wave aberrations to the subjects, we demonstrated that the best subjective image quality occurs when some aberrations are left uncorrected. This result also supports the hypothesis that the neural visual system is adapted to his specific pattern of retinal image blur. The apparent adaptation to higher order aberrations reported here may reflect the process by which presbyopic patients become accustomed to bifocals, where the seamless transition from one power to the next introduces not only distortion but also higher order aberrations. Patients are advised of this and told they are more likely to adapt to the increase in aberrations if they put on the glasses and wear them for 2 weeks during all waking hours.

Our results also show that this adaptation is far from complete in that the best image quality occurs with 88% rather than 100% of the subject's original aberrations removed. This result for high order aberrations is roughly similar to the clinical rule of thumb for assisting patients in tolerating a large astigmatic shift in their refraction: the patient is adapted to the full correction in at least two steps, with the first step being to correct about 75% of the astigmatism, not very different from the 87% correction that optimizes image quality for higher order aberrations. The

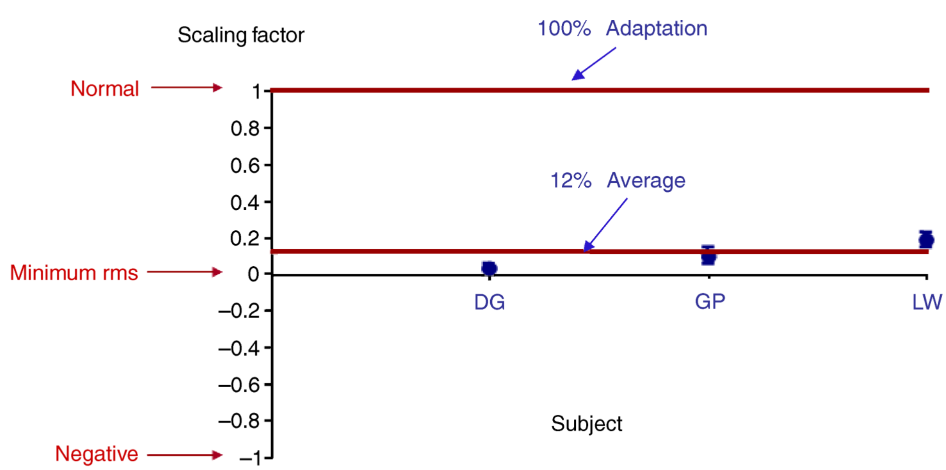

Figure 5. Result from the method of adjustment averaged across the three subject's measurements.

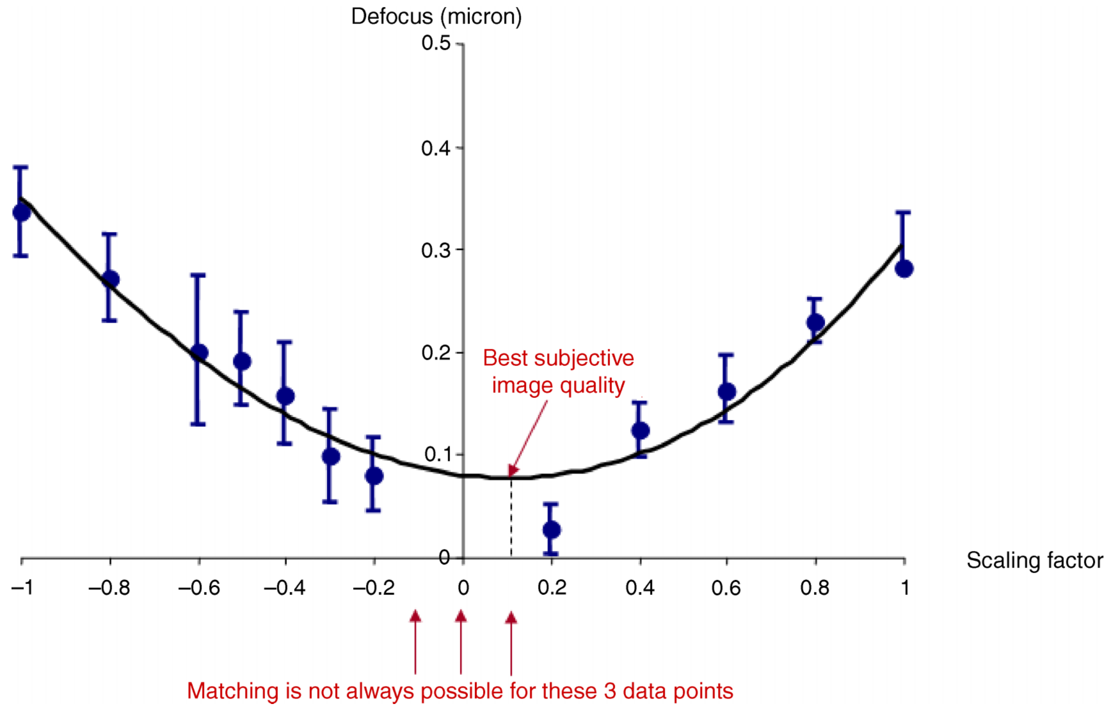

Figure 6. Results from blur matching with defocus, averaged across the three subject's measurement. The black curve is the best fit to the average measurement.

patient is asked to return in approximately 6 months to have their lenses updated as they adapt to the correction. At the second visit, the patient is refracted and typically the full correction is given to most of the patients.

There are several reasons why the small neural shift we measured here may not generalize to other situations. First, the amount of shift may depend on the nature of the visual stimulus used. We chose a high contrast stimulus with edges at all orientations to encourage the detection of subtle blur effects, but we have not tried other stimuli such as natural scenes, to see whether the amount of the neural shift is stimulus dependent. Second, to avoid potential artifacts from the limited stroke of our deformable mirror, we selected subjects with small amounts of higher order aberrations, averaging about 0.40 μm across a 6-mm pupil. The small aberrations of these subjects presumably placed modest demands on the plastic neural mechanisms that compensate for them. It is not known whether much larger shifts could be observed in individuals with much larger amounts of aberrations.

If larger shifts do occur, this adaptation phenomenon may have important implications for customized vision correction with contact lenses or refractive surgery. This effect will reduce the immediate benefit for the patient of attempts to produce diffraction-limited eyes. If the brain is adapted to a particular aberration pattern, when this is changed by the surgery or contact lens, the neural compensation will remain adjusted to the first aberration pattern for some time. The importance of this will depend on the time required to reverse the previous neural adaptation. We have not shown whether the shift we report here disappears following longer visual experience with fully corrected optics. In our previous experiments, we found that the visual system can adapt to a rotated pattern in a relatively short time of 15 min (Artal, Chen, Manzanera, & Williams, 2004). Patients, such as those with keratoconus, who have amounts of higher order aberrations an order of magnitude or more higher than normal, may not immediately favor complete removal of all higher order aberrations, and a sequenced customized correction may be useful in that case as it is in helping patients tolerate a large astigmatic shift. In eyes with modest higher order aberrations, customized contact lenses or refractive surgery will achieve very close to the best subjective image quality by correcting all the aberrations.

Conclusions

We have shown that the best subjective image quality does not necessarily occur when the quality of the retinal image is highest. Neural adaptation slightly modified the best aberration correction, although this effect averaged only about 12% of complete adaptation from our three observers. Moreover, the effect may well disappear following longer visual experience with fully corrected optics. Neural adaptation is neither large enough nor probably permanent enough to warrant partial instead of complete correction of the eye's aberrations with customized contact lenses or refractive surgery, at least in eyes with normal amounts of higher order aberrations. However, judging from clinical experience with tolerance to astigmatic shifts, it is likely that larger neural shifts occur in eyes with larger amounts of higher order aberrations, in which case this phenomenon may have implications for the delivery of vision correction.

Acknowledgments

This work has been supported in part by the National Science Foundation Science and Technology Center for Adaptive Optics, managed by the University of California at Santa Cruz under cooperative agreement No. AST-9876783 and through the National Eye Institute, and grant No. 8PEY001319; and the Spanish Ministry of Education and Science (grant FIS2004-2153).

David Williams is an inventor on patents on adaptive optics licensed to Bausch and Lomb and Optos, Inc.

Corresponding author: Li Chen.
E-mail: li.chen@amo-inc.com.
Address: Advanced Medical Optics, Inc., 3400 Central Expressway, Santa Clara, CA 95051.

References

ANSI Z136.1 American National Standard for the Safe Use of Lasers. (1993). Orlando: Laser Institute of America.

Artal, P., Chen, L., Fernández, E. J., Singer, B., Manzanera, S., & Williams, D. R. (2004). Neural compensation for the eye's optical aberrations. *Journal of Vision, 4*(4):4, 281–287, http://journalofvision.org/4/4/4/, doi:10.1167/4.4.4. [PubMed] [Article]

Artal, P., Chen, L., Manzanera, S., & Williams, D. R. (2004). Temporal dependence of neural compensation for the eye's aberrations. *Investigative Ophthalmology and Visual Science, 45,* 1077.

Artal, P., Guirao, A., Berrio, E., & Williams, D. R. (2001). Compensation of corneal aberrations by the internal optics in the human eye. *Journal of Vision, 1*(1):1, 1–8, http://journalofvision.org/1/1/1/, doi:10.1167/1.1.1. [PubMed] [Article]

Campbell, M. C., Harrison, E. M., & Simonet, P. (1990). Psychophysical measurement of the blur on the retina due to optical aberrations of the eye. *Vision Research. 30,* 1587–1602. [PubMed]

Chen, L., Singer, B., Guirao, A., Porter, J., & Williams, D. R. (2005). Image metrics for predicting subjective image quality. *Optometry and Vision Science, 82,* 358–369. [PubMed]

Fernández, E. J., Iglesias, I., & Artal, P. (2001). Closed-loop adaptive optics in the human eye. *Optics Letters, 26,* 746–748.

George, S., & Rosenfield, M. (2004). Blur adaptation and myopia. *Optometry and Vision Science, 81,* 543–547. [PubMed]

He, J. C., Marcos, S., Webb, R. H., & Burns, S. A. (1998). Measurement of the wavefront aberration of the eye by a fast psychophysical procedure. *Journal of the Optical Society of America A, Optics, image science, and vision, 15,* 2449–2456. [PubMed]

Helmholtz, H. V. (1881). Popular lectures on scientific subjects: Second series. London: Longmans, Green.

Hofer, H., Artal, P., Singer, B., Aragón, J. L., & Williams, D. R. (2001). Dynamics of the eye's wave aberration. *Journal of the Optical Society of America A, Optics, image science, and vision, 18,* 497–506. [PubMed]

Hofer, H., Chen, L., Yoon G. Y., Yamauchi, Y., & Williams, D. R. (2001). Improvement in retinal image quality with dynamic correction of the eye's aberration. *Optics Express, 8,* 631–643.

Howland, H. C., & Buettner, J. (1989). Computing high order wave aberration coefficients from variations of best focus for small artificial pupils. *Vision Research, 29,* 979–983. [PubMed]

Howland, H. C., & Howland, B. (1977). A subjective method for the measurement of monochromatic aberrations of the eye. *Journal of the Optical Society of America, 67,* 1508–1518. [PubMed]

Iglesias, I., Berrio, E., & Artal, P. (1998). Estimates of the ocular wave aberration from pairs of double-pass retinal images. *Journal of the Optical Society of America A, Optics, image science, and vision, 15,* 2466–2476. [PubMed]

Liang, J., Grimm, B., Goelz, S., & Bille, J. F. (1994). Objective measurement of wave aberrations of the human eye with the use of a Hartmann–Shack wavefront sensor. *Journal of the Optical Society of America A, Optics, image science, and vision, 11,* 1949–1957. [PubMed]

Liang, J., & Williams, D. R. (1997). Aberrations and retinal image quality of the normal human eye. *Journal of the Optical Society of America A, Optics, image science, and vision, 14,* 2873–2883. [PubMed]

Liang, J., Williams, D. R., & Miller, D. T. (1997). Supernormal vision and high-resolution retinal imaging through adaptive optics. *Journal of the Optical Society of America A, Optics, image science, and vision, 14,* 2884–2892. [PubMed]

Mierdel, P., Krinke, H. E., Wiegand, W., Kaemmerer, M., & Seiler, T. (1997). Measuring device for determining monochromatic aberration of the human eye. *Ophthalmology, 94,* 441–445. [PubMed]

Mon-Williams, M., Tresilian, J. R., Strang, N. C., Kochhar, P., & Wann, J. P. (1998). Improving vision: neural compensation for optical defocus. *Proceedings of the Royal Society B: Biological Sciences, 265,* 71–77. [PubMed] [Article]

Navarro, R., & Losada, M. A. (1997). Aberrations and relative efficiency of light pencils in the living human eye. *Optometry and Vision Science, 74,* 540–547. [PubMed]

Pesudovs, K., & Brennan, N. A. (1993). Decreased uncorrected vision after a period of distance fixation with spectacle wear. *Optometry and Vision Science, 70,* 528–531. [PubMed]

Roorda, A., & Williams, D. R. (1999). The arrangement of the three cone classes in the living human eye. *Nature, 397,* 520–522. [PubMed]

Rosenblum, W. M., & Christensen, J. L. (1976). Uncorrected myopes exhibit significant blur adaptation. *Optometry and Vision Science, 13,* 69–91.

Rosenfield, M., & Hong, S. (2001). Uncorrected myopes exhibit significant blur adaptation. *Optometry and Vision Science, 78,* 87.

Rosenfield, M., Hong, S. E., & George, S. (2004). Blur adaptation in myopes. *Optometry and Vision Science, 81,* 657–662. [PubMed]

Smirnov, M. S. (1961). Measurement of the wave aberration of the human eye. *Biofizika, 6,* 687–703. [PubMed]

Van den Brink, G. (1962). Measurements of the geometrical aberrations of the eye. *Vision Research, 2,* 233–244.

Walsh, G., Charman, W. N., & Howland, H. C. (1984). Objective technique for the determination of monochromatic aberrations of the human eye. *Journal of the Optical Society of America A, Optics and image science, 1,* 987–992. [PubMed]

Watt, R. J. (1987). An outline of the primal sketch in human vision. *Pattern Recognition Letters, 5,* 139–150.

Webster, M. A. (2005). Adaptation and Visual Experience. *Optics and Photonics News, 16,* 18–23.

Webster, M. A., Georgeson, M. A., & Webster, S. M. (2002). Neural adjustments to image blur. *Nature Neuroscience, 5,* 839–840. [PubMed] [Article]

Williams, D. R., Liang, J., Miller, D., & Roorda, A. (1999), Wavefront sensing and compensation for the human eye. In R. K. Tyson (Ed.), *Adaptive Optics Engineering Handbook* (pp. 287–310). New York: Marcel Dekker.

Young, T. (1801). The Bakerian Lecture. On the mechanism of the eye. *Philosophical Transactions of the Royal Society of London Part 1, 91,* 23–88.